ocument Room, DOCUMENT ROOM 36-412
esearch Laboratory of Electronics
assachusetts Institute of Technology

#3

PRINTED MICROWAVE SYSTEMS

MARTIN SCHETZEN

LOAN COPY only

TECHNICAL REPORT 289

SEPTEMBER 30, 1954

RESEARCH LABORATORY OF ELECTRONICS
MASSACHUSETTS INSTITUTE OF TECHNOLOGY
CAMBRIDGE, MASSACHUSETTS

The Research Laboratory of Electronics is an interdepartmental laboratory of the Department of Electrical Engineering and the Department of Physics.

The research reported in this document was made possible in part by support extended the Massachusetts Institute of Technology, Research Laboratory of Electronics, jointly by the Army Signal Corps, the Navy Department (Office of Naval Research), and the Air Force (Office of Scientific Research, Air Research and Development Command), under Signal Corps Contract DA36-039 sc-42607, Project 132B; Department of the Army Project 3-99-12-022.

MASSACHUSETTS INSTITUTE OF TECHNOLOGY

RESEARCH LABORATORY OF ELECTRONICS

Technical Report 289 September 30, 1954

PRINTED MICROWAVE SYSTEMS

Martin Schetzen

This report is based on a thesis submitted in partial fulfillment of the requirements for the degree of Master of Science, Department of Electrical Engineering, M.I.T., 1954.

Abstract

The results of a theoretical and experimental investigation of the free modes that propagate on the strip transmission line are reported. A Fourier integral solution is obtained for the free modes. Since the integrals must be solved by numerical methods, approximate equations for the phase velocity, attenuation, and the characteristic impedance are developed for the "two-conductor" H-E mode. It is shown that a static assumption for the H-E mode is good only as a first approximation. In the course of the discussion, it is proved that the only free modes that may exist on any n-conductor system of arbitrary but constant cross section in homogeneous and simply connected space are TEM modes.

Previously known methods for the determination of the guide wavelength and attenuation required that the standing waves of the strip transmission line be known. It was found that these could not be measured directly. Since precedent measuring methods were found to be inadequate, a new simple method for measuring the attenuation of any transmission line through a junction is presented.

I. INTRODUCTION

Conventional microwave systems are bulkier, heavier, and costlier than is desirable in applications to airborne equipment. These limitations have prompted the investigation of various types of miniaturized microwave systems. If such a structure is to be an acceptable substitute for present-day systems, it should possess the following properties:

(1) The ohmic and dielectric losses should be low for efficient transmission of power.

(2) The radiation must be negligibly small to achieve low cross talk.

(3) The fields of the dominant mode must be confined to a small region about the system so that the system will be electrically and physically small.

(4) The system should propagate energy in essentially only one mode for simplicity of design within the desired frequency band.

(5) For ease in production, the transmission line should not be critical to small changes in the physical constants of the system.

The proposed structure should also be lightweight and compact.

The conventional microwave transmission systems are the waveguide and coaxial line. Although the waveguide has good electrical properties, it does not fulfill the requirements given above because of its bulk, expense, and weight. The coaxial line does not meet the requirements because of its high cost and high loss for miniature sizes (approximately 0.6 db/ft at S-band frequencies with teflon dielectric). Also, both systems require couplings at every junction; this requirement increases the loss of the junction, narrows its bandwidth, and greatly increases the cost of production.

One of the first proposed miniature microwave transmission lines was the dielectric coated wire (the Goubau line), which propagates energy as surface waves somewhat similar to the Sommerfeld wave (1). Although this structure is physically small and has a low attenuation, it does not meet the criteria set forth: the fields of the dominant E-mode are not confined to a small region about the wire, making the line electrically large; a discontinuity will cause radiation, making it difficult to support the line and increasing cross talk.

With none of these structures can a given microwave network be mass-produced cheaply and simply. Printed circuits, since their introduction early in 1945 for low-frequency application, have been demonstrated to be amenable to efficient and cheap manufacture. Thus, a microwave structure which could be produced by conventional printed circuit techniques would be desirable.

Several types of printed microwave transmission lines have been suggested. Among the proposed structures are: the "dielectric sandwich" (2), which consists of a conducting metal strip separated from parallel ground planes on either side of it by dielectric sheets (Fig. 1); the "high-Q line" (3), which consists of conducting metal strips placed on either side of a thin dielectric sheet supported between two parallel ground planes (Fig. 2); the "air-strip line" (4), which consists of a metal strip supported above

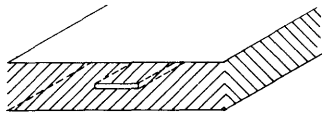

Fig. 1
Sandwich line.

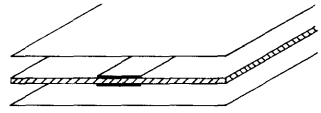

Fig. 2
High-Q line.

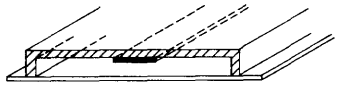

Fig. 3
Air-strip line.

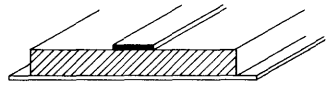

Fig. 4
Microstrip line.

a ground plane by a dielectric sheet above the strip (Fig. 3); and the "strip line" (5), in which a metal strip is separated from a ground plane by a dielectric sheet (Fig. 4). The major purpose of this report is to contribute to the analysis of the electrical properties of the strip line.

II. SURFACE WAVES

Before a mathematical analysis is given, a heuristic analysis of the structure will present some knowledge of the types and the characteristics of the free modes that may be expected to propagate on such a structure. By "free (or natural) modes" will be meant those modes whose propagation constants, γ_n, are determined solely by the geometrical and electrical constants of the system.

Consider, first, the strip line (Fig. 4) with the conducting metal strip removed. The types of free modes that this type of structure will support may be studied from an analysis of an infinite ground plane covered with a dielectric sheet of thickness, d. The free modes for such a structure are surface waves whose fields decay exponentially from the surface of the dielectric sheet (6, 7). As opposed to closed boundary structures, the dominant surface-wave mode is an E-mode that may propagate down to zero frequency. Also, for decreasing frequency, dielectric thickness, or dielectric constant, the longitudinal component of the field decreases more rapidly than the transverse components, and the exponential decay of the fields from the surface of the dielectric sheet is less rapid (4). Thus, the wave approaches a plane wave, and the energy distributes itself more evenly over all space. Therefore, as the frequency, dielectric thickness, or dielectric constant is decreased, the surface-wave E-mode becomes more difficult to excite, and the coupling of a given antenna (such as a conducting metal strip on the surface of the dielectric) to this mode decreases.

The next order surface-wave mode that may propagate is an H-mode. This mode will begin to propagate at a frequency $\omega_d = c/d\chi^{1/2}$, where c is the velocity of light in

free space (3×10^8 meters/second), d is the thickness of the dielectric sheet, χ is the electric susceptibility of the dielectric sheet, and ω_d is the divergence frequency of the H-mode. The term divergence frequency is used instead of cut-off frequency because below this frequency the mode does not exist; that is, there are no H-mode solutions of Maxwell's equations (8). This is as opposed to closed boundary structures, where the mode still exists below its cut-off frequency but with a real propagation constant.

Thus, if for a given maximum frequency and dielectric constant it is desired that no higher order surface waves exist, the dielectric thickness must be less than

$$d = \frac{c}{\omega_d \chi^{1/2}} \tag{1}$$

III. THE H-E MODE

In addition to perturbing the surface waves, a conducting metal strip will introduce a "two-conductor" mode. This is the free mode of main interest, since its fields should be confined to a small region about the strip. It is recognized that this mode will be a TEM mode perturbed by the presence of the dielectric sheet, for it is proved in Appendix III that the only possible types of free modes on parallel-wire transmission lines are TEM modes. Thus, if the electric susceptibility of the dielectric sheet were zero, the TEM mode would be the only type of free mode that could exist. As the electric susceptibility is increased, in addition to introducing the perturbed surface waves, the TEM mode will be perturbed, and both longitudinal E and H fields will be introduced. The "two-conductor" mode should thus be more properly called an H-E mode. However, since most of the energy of the wave may be expected to be within the dielectric sheet, the H-E mode may be expected to retain many of the properties of a TEM wave. (It will be shown later that for the cases of interest, approximately 90 per cent of the total energy of the wave is in the dielectric sheet.)

A. THE PHASE VELOCITY OF THE H-E MODE

For example, since the phase velocity of a TEM wave is independent of frequency, the phase velocity of the H-E mode may be expected to be essentially constant with respect to frequency. This expectation has been experimentally verified by measurements of the guide wavelength over a range of frequencies of 3-10 kMc/sec for various strip widths and dielectric thicknesses (Fig. 5). Since this graph is in hyperbolic coordinates, the phase velocity is proportional to the slope and may therefore be written as

$$V_\theta = \frac{c}{K_e^{1/2}} \tag{2}$$

where K_e is defined as an effective dielectric constant. Also note that all the graphs pass through the origin. Since the field solution of the H-E mode must approach the

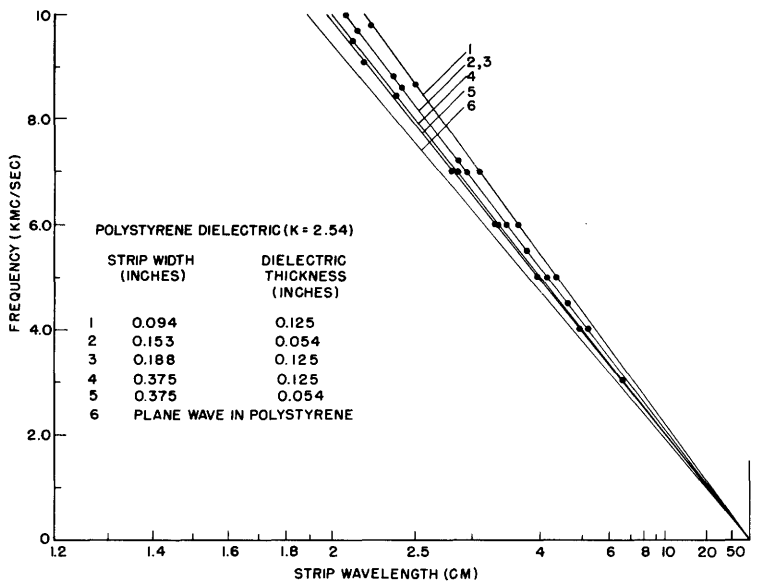

Fig. 5
Guide wavelength of the dominant H-E mode vs. frequency.

static field solution as the frequency approaches zero, the phase velocity may be expected to be given by

$$V_\theta = \frac{1}{(LC)^{1/2}} \tag{3}$$

where L is the inductance per unit length, and C is the capacitance per unit length. Since the presence of the dielectric does not affect the inductance, the expression may be written as

$$V_\theta = \frac{1}{(LaC_o)^{1/2}} = \frac{c}{a^{1/2}} \tag{4}$$

where $a = C/C_o$ is the ratio of the capacitance per unit length with the dielectric sheet present to the capacitance per unit length with the dielectric sheet removed. If Eq. 4 is true, then from Eq. 2 it is required that

$$a = K_e \tag{5}$$

The quantity C_o may be computed exactly by conformal mapping techniques (9) and is given by the equations

$$C_o = \frac{203.2}{12\pi} \frac{K'}{K} \tag{6}$$

$$R = \frac{4}{\pi} [K' E' (\beta, k) - E' F' (\beta, k)] \tag{7}$$

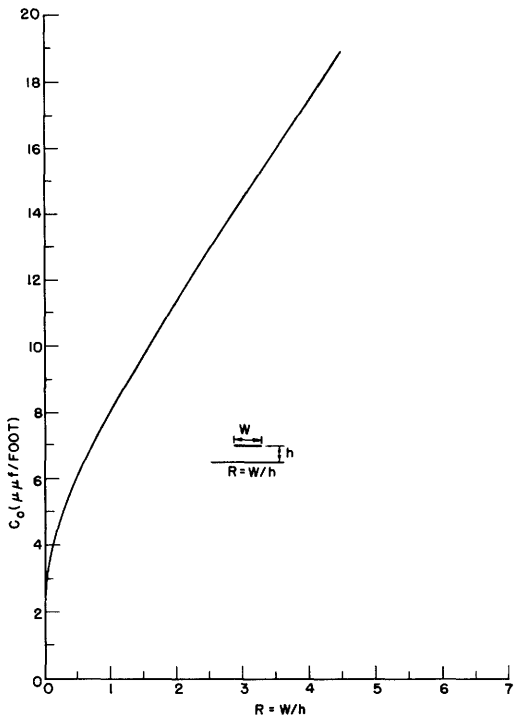

Fig. 6

Capacitance per unit length of a strip above a ground plane.

where $\sin^2 \beta = (K' - E')/[K'(1 - K^2)]$ and

C_o is the capacitance in micromicrofarads per foot

R is the ratio of the strip width to the height of the strip above the ground plane

k is the modulus of the elliptic integrals

K is the complete elliptic integral of the first kind

K' is the complete complementary integral of the first kind

E' is the complete complementary integral of the second kind

$F'(\beta, k)$ is the complementary elliptic integral of the first kind

$E'(\beta, k)$ is the complementary elliptic integral of the second kind.

A plot of C_o vs. R is given in Fig. 6. The capacitance, C, per unit length with the dielectric sheet present may also be computed by conformal mapping techniques (10); but since the equations become extremely complicated and difficult to solve, it was measured on a capacitance bridge instead of being computed. Table I shows that the agreement between a and K_e is within 1 per cent, which is within experimental error. Thus, it has been verified that the phase velocity may be determined by static considerations and is given by Eq. 3.

Since the phase velocity may be determined by static considerations, one might expect that the fields of the H-E mode would look very much like the static fields, and that all other parameters could be determined by static considerations. However, care must be taken in this line of thought because the phase velocity is determined by an

Table I

Strip width (inches)	Polystyrene dielectric thickness (inches)	K_e	a
0.375	0.125	2.23	2.25
0.188	0.125	2.10	2.09
0.094	0.125	1.94	1.95
0.375	0.054	2.32	2.3
0.153	0.054	2.10	2.11

integral of the fields over the complete cross section. Thus, one may be incorrect in his assumption of the fields by a considerable amount and yet he may calculate the correct phase velocity from the assumed field pattern. For example, the H_{on} and the E_{1n} modes in a circular waveguide both have the same cut-off frequency and phase velocity, and yet their field patterns and other parameters (such as attenuation and impedance) are entirely different. Hence, one may not say a priori that because the phase velocity may be determined by static considerations, the field pattern and all other parameters may be determined by such an assumption.

In order to check the validity of the static field assumption for the H-E mode, a mathematical analysis is required. One method of solution is to expand the fields into some complete set so that each component is a solution of Maxwell's equations. This set may then be summed in such a manner that the boundary conditions are satisfied. In the search for an appropriate set, a series was chosen for which each component satisfied the boundary conditions for a sinusoidal current distribution on the surface of the dielectric without the strip. A Fourier integral of all such currents was then formed so that it represented the fields caused by a current that is different from zero only over the region occupied by the strip. Since the strip was assumed to be narrow as compared with a wavelength, it sufficed to make the tangential component of the electric field zero only at the center of the strip.

The details of this analysis are given in Appendix III. In the analysis, no transverse currents were assumed to exist in the strip. This approximation follows from the assumption that the strip is narrow as compared with a wavelength. For, if transverse currents do exist in the strip, they will be zero at each edge of the strip, and they cannot differ very much from zero at any place in the strip. The assumptions made in the analysis thus become more exact as the width of the strip in wavelengths is decreased.

From this analysis, the propagation constant may be determined by calculating the roots of Eq. III-39. Calculations at several frequencies and for several geometries have been found to check with the measured values within experimental error of 1 per cent. The fields may then be calculated from Eqs. III-40 and III-41. If a static field is assumed, these calculations indicate that the static field will reasonably approximate

Fig. 7
Regions of valid static field approximation for the H-E mode.

the H-E mode in region A of Fig. 7, but within region B the transverse fields become of the same order of magnitude as the longitudinal fields. Thus, the static field assumption may be used only as a first approximation in the design of strip line components.

B. THE CHARACTERISTIC IMPEDANCE OF THE H-E MODE

For structures in homogeneous media (such as waveguides), it is usual to define the characteristic impedance as the ratio of the transverse electric field to the transverse magnetic field. Since the strip transmission line is only regionally homogeneous, this ratio will be a function of position and thus its use will be of little value. Instead, the definition that will be adopted is

$$Z_o = \frac{V}{I} \tag{8}$$

where I is defined as the total longitudinal current in the strip, and V is the integral of the electric field from the ground plane to the strip along the axis of symmetry of the cross section (the path a-b shown in Fig. 8). This definition is particularly useful when the strip line is thought of as being fed by a source between the "terminals" a-b. The integral equation for the characteristic impedance defined by Eq. 8 is given in Appendix IV. It is noted there that the arbitrary factor, N, has been set equal to unity; thus, the low-frequency impedance will differ from that calculated from the equation $Z_o = 1/cC_o(K_e)^{1/2}$ by a normalization factor.

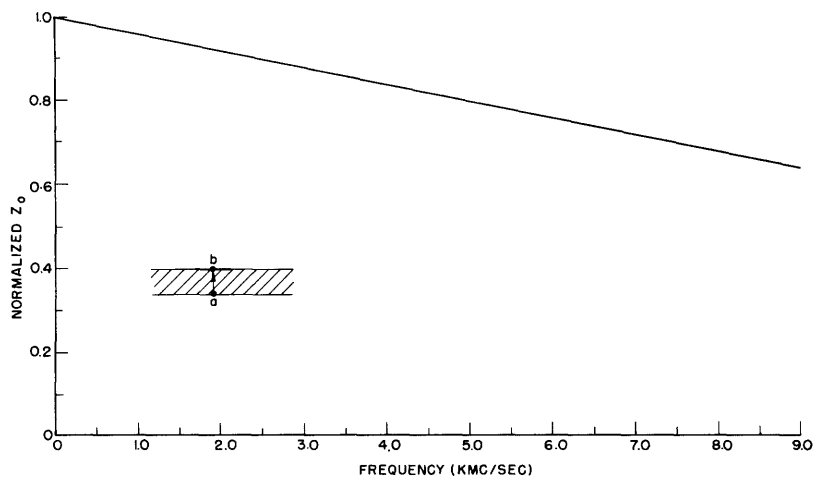

Fig. 8
Characteristic impedance of the microstrip line as a function of frequency.

Figure 8 shows the variation of the characteristic impedance with frequency up to 10 kMc/sec for a strip line with polystyrene as the dielectric sheet (K = 2.54). It is observed that the characteristic impedance, contrary to what may be expected from static considerations, decreases approximately linearly with frequency. Although the decrease in impedance is quite small over limited ranges of frequency (less than 1000 Mc/sec), it is appreciable over extended frequency ranges. The impedance, it is further observed from Fig. 8, decreases at a rate of approximately 4 per cent per thousand megacycles independently of the zero frequency impedance. Thus, for a strip line with a polystyrene dielectric sheet, the impedance may be written as

$$Z_o = \frac{1}{cC_o(K_e)^{1/2}} \left[1 - 40 \times 10^{-6} f\right] \qquad f \leq 10 \text{ kMc/sec} \qquad (9)$$

where f is the frequency in megacycles per second.

C. THE ATTENUATION OF THE H-E MODE

In addition to dielectric and ohmic losses, there will be some energy loss caused by coupling to the surface-wave E-mode and radiation of the line. Since any finite open-boundary structure must radiate (11), the radiation losses of the strip transmission line may not be completely eliminated, but by keeping the spacing between the strip and the ground plane small as compared with the wavelength (less than one-tenth of a wavelength) it has been found that the radiation is negligibly small. From the previous discussion on surface waves, it is seen that the coupling to the surface-wave E-mode may be reduced by decreasing the separation between the strip and the ground plane and by using dielectric materials with low dielectric constants. Under these restrictions, one may then expect that the main losses will be the dielectric and ohmic losses.

Because of the difficulty in solving the integral equations of Appendix III for the fields of the H-E mode, they were not used to determine the attenuation. Instead, the attenuation for a strip transmission line with polystyrene as the dielectric was measured at several frequencies and for several geometries. The measurements were made by the techniques described in Section IV. It will be observed that the attenuation, as measured in this manner, includes not only the dielectric and ohmic losses as losses charged to the H-E mode, but also the energy lost through the coupling to the surface waves and the radiation of the line. Thus, the measured attenuation will not correspond exactly to the actual attenuation constant of the H-E mode. However, these measurements are realistic in the sense that the measured attenuation will determine the actual loss of available energy in the H-E mode. The results of the measurements are tabulated in Table II.

Also tabulated in Table II are the calculated values for the attenuation of a TEM wave that would propagate if all space were filled with the same dielectric material as that of the dielectric sheet below the strip. The approximate equations for this attenuation are

Table II

Strip width, 0.375 inch; polystyrene thickness, 0.125 inch; loss factor of polystyrene, 0.001.

Frequency (Mc/sec)	α_m(db/ft)	α_{TEM}(db/ft)
4800	0.3	0.3
5810	0.3	0.4
6810	0.5	0.5
7000	0.9	0.5
7570	0.9	0.5
8461	1.2	0.6

Strip width, 0.154 inch; polystyrene thickness, 0.054 inch; loss factor of polystyrene, 0.001.

Frequency (Mc/sec)	α_m(db/ft)	α_{TEM}(db/ft)
4000	1.0	0.4
6000	1.1	0.6
7000	1.4	0.7
8582	1.6	0.8

given (12) by

$$\alpha_{TEM} = \alpha_c + \alpha_d \qquad \alpha_d = 1/2\, \sigma_d (\mu/\epsilon)^{1/2}$$

$$\alpha_c \approx \frac{8.69}{d} (\omega\epsilon/2\sigma_c)^{1/2} \frac{1 + \frac{\pi}{2} R + \frac{\pi}{2} + \ln \frac{2}{\rho}}{1 + \frac{\pi}{2} R + \ln \left[1 + \frac{\pi}{2} R\right]} \text{ db/unit length} \tag{10}$$

where $\rho = [2\beta^2 - 1 + 2\beta(\beta^2 - 1)^{1/2}]$, $\beta = 1 + t/d$, $\sigma_d = \omega \tan \Phi$, σ_c is the conductivity of the conductors, $R = W/d$ is the ratio of the width to the height of the strip above the ground plane, and t is the thickness of the strip. By comparing the values for the attenuation of the TEM wave, α_{TEM}, with the measured attenuation of the H-E mode, α_m, it is observed that

$$\alpha_{TEM} \leq \alpha_m \leq 2\alpha_{TEM}$$

It is thus seen that α_{TEM} may be used as a first-order approximation for α_m. Also, since the measured attenuation increases for decreasing dielectric thickness, we may conclude that the energy lost from coupling to the surface-wave E-mode and radiation of the line is negligible as compared with the dielectric and ohmic losses.

D. GENERAL REMARKS ON THE H-E MODE

In the introduction it was pointed out that an essential property of a miniaturized microwave transmission line is that the fields of the dominant mode must be confined to a small region about the system. A measure of how well the fields of the H-E mode are confined would be the percentage of the total energy of the H-E mode that is within the dielectric region. By the use of a variational principle for the propagation constant of any cylindrical system (13), this percentage has been found to be given approximately by the equation (see Appendix V)

$$\frac{W_1}{W_t} = \frac{K}{\chi}\frac{\chi_e}{K_e} \tag{11}$$

where W_1/W_t is the ratio of the energy in the dielectric region to the total energy of the wave, $\chi = K - 1$ is the electric susceptibility of the dielectric sheet, and $\chi_e = K_e - 1$ is the "effective" susceptibility of the H-E mode.

From the values of K_e given in Table I, it is seen that approximately 90 per cent of the total energy is within the dielectric region. Thus, for the strip transmission line, the fields of the H-E mode are confined to a small region about the strip.

In summary, it has been found that the strip transmission line will support surface waves in addition to the desired "two-conductor" H-E mode whose fields are confined to a small region about the strip. However, if the dielectric sheet is kept less than the critical thickness given by Eq. 1, then the only surface-wave mode that may propagate is the E-mode. Although the coupling to this mode is small, it may be further decreased by using a lower dielectric constant or a thinner dielectric sheet under the strip. By measurement techniques to be described in Section IV, the phase velocity of the H-E mode has been found to be independent of frequency and may be determined from static considerations by Eq. 4. The attenuation has been found to be of the same order of magnitude as for coaxial cables and may be approximated by Eq. 10. By a mathematical analysis of the strip transmission line, however, it was determined that a static approximation of the fields may be used only as a first-order approximation to the actual fields of the H-E mode. Also, the characteristic impedance decreases with increasing frequency; it is given by Eq. 9 for a strip transmission line with polystyrene as the dielectric.

Thus, the strip transmission line is a desirable system in applications where low cost, compactness, and ruggedness are the prime considerations. For those applications where a higher Q system is desired, the air-strip line (Fig. 3) should be investigated.

IV. EXPERIMENTAL DETERMINATION OF THE PROPAGATION CONSTANT

A. MEASUREMENT OF THE STANDING WAVE

In developing and checking the theory of the strip line, the two quantities of main interest were the guide wavelength and the attenuation of the line. Conventional measurement techniques depend, for the determination of these quantities, upon the measurement of the standing waves along the line. However, as was shown in Section II, in addition to the fields of the desired H-E mode, the fields about the strip line will be composed of undesired radiation and surface-wave fields. These undesired fields decay much less rapidly from the surface of the dielectric than those of the H-E mode. Thus, even though there is relatively little energy in the undesired fields, a short distance from the strip, their magnitude will be of the same order as that of the fields of the desired H-E mode. Any measurement, therefore, of the fields above the strip line will result in a complex beat pattern and not the desired standing-wave pattern of the H-E mode (Fig. 9). Conventional measurement techniques are thus not suitable for the determination of the guide wavelength or the attenuation of the strip line, since they depend upon a knowledge of the standing waves of the mode for which these quantities are desired.

B. MEASUREMENT OF THE INPUT IMPEDANCE

Since only the fields of the H-E mode will be concentrated about the strip, a small discontinuity on top of the strip may be expected to scatter mainly the H-E mode and only negligibly the other fields. Thus, a possible method of measuring the desired

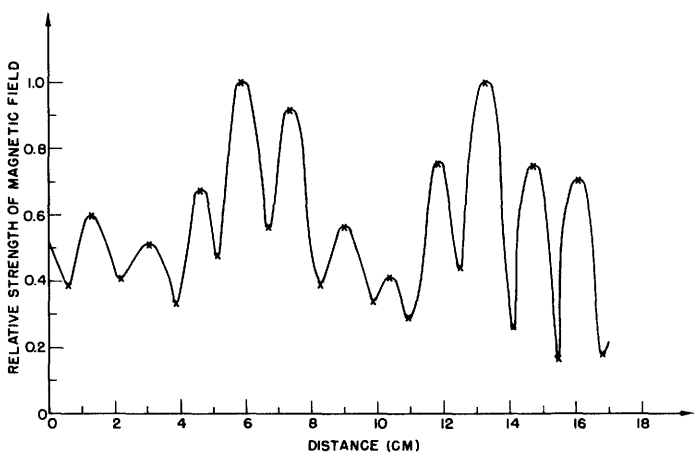

Fig. 9

Distribution of magnetic field along the strip. Strip width, 3/8 inch; polystyrene sheet thickness, 1/8 inch; frequency, 10 kMc/sec.

quantities would be to measure the variation of the input impedance to the line as a small discontinuity is moved along the strip with the line terminated in a matched load. A plot of the input impedance on a Smith chart as the discontinuity is moved would be a circle centered at the point (1 + j0). How well the points lie on a circle would be a measure of how much of the surface-wave E-mode was also reflected. Twice the distance that the discontinuity was moved to complete the circle would correspond to the guide wavelength. If the measurements were then repeated with the discontinuity a distance L further from the source, another circle would be obtained with the same center but with a smaller radius than the first. The attenuation would be given by

$$\alpha L = 1/2 \ln \frac{R_2}{R_1} \text{ nepers} \tag{12}$$

where R_2 and R_1 are the radii of the larger and smaller circles, respectively. However, the input impedance to the line cannot be measured directly, since this would require a knowledge of the standing waves of the H-E mode, which cannot be directly measured. If the strip line were fed by a coaxial cable, for example, it would not suffice to measure the standing waves in the coaxial line: the junction between the coaxial line and the strip line would not necessarily be reflectionless and the circle diagrams would be altered. The usual procedure involved when such difficulties arise (which occurs in practically all such measurements) is to determine the impedance matrix characterizing the junction and then calculate the impedance of the load terminating the junction from measurement of the input impedance of the junction and the load. This procedure is laborious and requires a knowledge of all the impedance elements representing the four-terminal network of the junction, even though they are not desired. From a study of the general properties of two-port junctions, a method has been developed by which the attenuation and the guide wavelength may be determined in a simple manner from a few measurements, without the necessity of determining any of the junction's scattering matrix elements.

C. THE SCATTERING MATRIX OF A JUNCTION

Consider a junction between any two guiding systems, indicated symbolically in Fig. 10. The two systems do not need to be identical. For example, one could be a coaxial line or waveguide; the other, the strip line. If the junction is linear, it may be

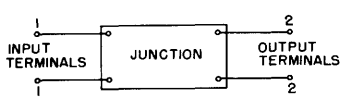

Fig. 10
Schematic representation of a two-port junction.

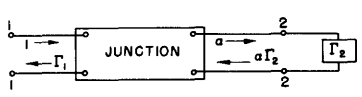

Fig. 11
A two-port junction terminated by a load, Γ_2.

completely described by the scattering matrix, S, of the junction

$$[S] = \begin{bmatrix} S_{11} & S_{12} \\ S_{21} & S_{22} \end{bmatrix}$$

where the matrix elements have the following definitions:

S_{11} is the reflected wave at terminal 1 resulting from a unit wave incident at terminal 1 when the junction is matched at terminal 2.

S_{12} is the transmitted wave at terminal 2 resulting from a unit wave incident at terminal 1 when the junction is matched at terminal 2.

S_{22} is the reflected wave at terminal 2 resulting from a unit wave incident at terminal 2 when the junction is matched at terminal 1.

S_{21} is the transmitted wave at terminal 1 resulting from a unit wave incident at terminal 2 when the junction is matched at terminal 1.

To determine how the junction alters the circle diagrams suppose that the junction is terminated in a load characterized by a reflection coefficient, Γ_2. The reflection coefficient, Γ_1, measured at the input terminals, may then be expressed in terms of Γ_2 and the elements of the scattering matrix, S. Figure 11 is a schematic representation of this condition. The arrows indicate the directions of propagation for a unit wave incident at terminal 1. The total outward wave at terminal 2 is denoted by α. The wave incident on terminal 2 is therefore $\alpha\Gamma_2$; that reflected from the input is Γ_1. Thus, from the definitions of S_{ij} given above, there follows

$$\alpha = S_{12} \cdot 1 + S_{22} \cdot \alpha\Gamma_2 \tag{13}$$

and

$$\Gamma_1 = S_{11} \cdot 1 + S_{12} \cdot \alpha\Gamma_2 \tag{14}$$

Solving Eqs. 13 and 14 for Γ_1, we have

$$\Gamma_1 = \frac{S_{11} + (S_{12}S_{21} - S_{11}S_{22})\,\Gamma_2}{1 - S_{22}\Gamma_2} \tag{15}$$

This is a relation between two complex numbers, Γ_1 and Γ_2, of the form

$$W = \frac{AZ + B}{CZ + D} \tag{16}$$

where W and Z are complex variables, and A, B, C, and D are complex constants. It is recognized that Eq. 16 is a linear fractional transformation that maps the Z-plane into the W-plane (14). Some of the well-known properties of this type of transformation required for our discussion are:

a. If straight lines are considered as limiting cases of circles, the linear fractional transformation maps circles in the Z-plane into other circles in the W-plane, generally

with different radii and centers.

b. The mapping of points from the Z-plane into the W-plane is conformal. That is, if two curves in the Z-plane intersect at a given angle, their images in the W-plane will intersect at the same angle and with the same sense.

c. There exists a one-to-one correspondence between the Z-plane and the W-plane.

d. The cross ratio is invariant. That is, if four points, Z_1, Z_2, Z_3, and Z_4, in the Z-plane, and their images, W_1, W_2, W_3, and W_4, in the W-plane, are considered, the ratio

$$X = \frac{(Z_3 - Z_1)(Z_4 - Z_2)}{(Z_3 - Z_2)(Z_4 - Z_1)} = \frac{(W_3 - W_1)(W_4 - W_2)}{(W_3 - W_2)(W_4 - W_1)} \tag{17}$$

is invariant under the mapping of the form of Eq. 16.

D. THE CROSS-RATIO METHOD OF MEASURING ATTENUATION

From these properties of linear fractional transformations, certain effects of the junction upon the circle diagrams immediately become evident. Refer to Fig. 12. When a load with a reflection coefficient

$$\Gamma_L = \gamma_L \exp(j\Phi_L)$$

is viewed through a transmission line of length s and propagation constant $j\gamma = \alpha + j\beta$,

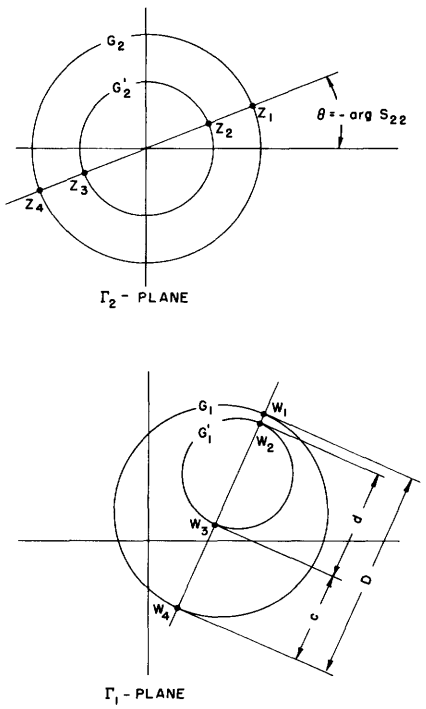

Fig. 12

Original circles in the Γ_2-plane; transformed circles in the Γ_1-plane.

the reflection coefficient seen at the input to the line is

$$\Gamma_2 = \gamma_L \exp(-2\alpha s) \exp[j(\Phi_L - 2\beta s)]$$

Thus, as s is varied by a half wavelength, a circle G_2 is obtained on the Smith chart about the point 1 + j0 and radius $R_2 = \gamma_L e^{-2\alpha s}$.* If Γ_2 is mapped by the linear fractional transformation of Eq. 15 (that is, when the measurements are made through a junction), the image points in the Γ_1-plane will also lie on a circle G_1 but with a different center and radius. However, since there exists a one-to-one correspondence between the Γ_2-plane and the Γ_1-plane, varying s by a half wavelength will also complete the circle in the Γ_1-plane. Thus, twice the distance that the discontinuity is moved to complete the circle as seen through the junction will correspond to the guide wavelength. If the load were now moved a distance L further down the transmission line, the reflection coefficient seen at the input to the line would be

$$\Gamma_2' = \gamma_L \exp[-2\alpha(L+s)] \exp\left\{j[\Phi_L - 2\beta(L+s)]\right\}$$

As s is varied, a second circle G_2' would be obtained in the Γ_2-plane with the same center as the first, but with a radius of $R_2' = \gamma_L e^{-2\alpha(L+s)}$. Thus, the ratio of the radii of the two circles in the Γ_2-plane is

$$\frac{R_2}{R_2'} = e^{2\alpha L} \tag{18}$$

If Γ_2' is now mapped by the same linear fractional transformation as Γ_2, a second circle G_1' in the Γ_1-plane would be obtained which would be smaller than but not concentric to the first. By the use of the invariance of the cross ratio, it will now be shown that the attenuation constant, α, may be determined without having to transform from the Γ_1-plane back into the Γ_2-plane (that is, without having to know the scattering matrix of the junction).

If the cross ratio is to be used, four separate points in the Γ_1-plane and their corresponding images in the Γ_2-plane must be chosen. Since the exact mapping is not known (that is, the scattering matrix elements of the junctions are not known), the corresponding images of points cannot be determined. However, from the property of conformality, since any diameter of the circles G_2 intersects G_2 orthogonally, its image in the Γ_1-plane must be an arc intersecting the circles G_1 orthogonally and in the same sense. The image of every diameter must be an arc with this property. In particular, if we let

$$\Gamma_2 = \rho \exp(j\theta) = \rho \exp(-j \arg S_{22})$$

---

*It is assumed here and for the rest of the discussion that the attenuation per one-half wavelength is negligibly small. If this were not true, a spiral instead of a circle would be obtained as s is varied. This condition, however, will be true for all transmission lines of practical interest.

so that Eq. 15 is written

$$\Gamma_1 = \frac{S_{11} + (S_{12}S_{21} - S_{11}S_{22})\rho \ \exp(-j \arg S_{22})}{1 - \rho \, |S_{22}|}$$

this particular diameter in the Γ_2-plane (ρ varying) will map into a straight line in the Γ_1-plane; thus, the diameter in the Γ_2-plane oriented so that $\theta = -\arg S_{22}$ maps into a straight line in the Γ_1-plane that intersects the circles G_1 orthogonally. This line in the Γ_1-plane can only be that line joining the centers of the two circles G_1.

Let the intersections in the Γ_1-plane be called W_1, W_2, W_3, and W_4, and let the points of intersection in the Γ_2-plane be called Z_1, Z_2, Z_3, and Z_4. Since the scattering matrix is unknown, the angle $\theta = -\arg S_{22}$ is unknown. It is also not known whether the image of W_1 is Z_1 or Z_4. However, in forming the cross ratio with these points, this knowledge is not required. For the moment, then, assume that the image of W_1 is Z_1. In the Γ_1-plane, the cross ratio is

$$X = \frac{(W_3 - W_1)(W_4 - W_2)}{(W_3 - W_2)(W_4 - W_1)} = \frac{(D-C)(d+C)}{Dd} \tag{19}$$

where D and d are the diameters of G_1 and G_1', respectively, and C is the distance between W_3 and W_4. In the Γ_2-plane, the cross ratio is

$$X = \frac{(Z_3 - Z_1)(Z_4 - Z_2)}{(Z_3 - Z_2)(Z_4 - Z_1)} = \frac{(R_2 + R_2')^2}{4 \, R_2 R_2'} = \frac{(1 + R_2/R_2')^2}{4 \, R_2/R_2'} \tag{20}$$

It is now observed that if the points Z_1, Z_2, Z_3, and Z_4, were relabeled Z_4', Z_3', Z_2', and Z_1', respectively, Eq. 20 would be unchanged. Thus, it is immaterial whether the image of W_1 is Z_1 or Z_4. Now, substituting Eq. 18 into Eq. 20, we obtain

$$X = \frac{[1 + \exp(2\alpha L)]^2}{4 \exp(2\alpha L)}$$

or

$$2X - 1 = \cosh 2\alpha L$$

Solving for αL, we obtain

$$\alpha L = 1/2 \cosh^{-1} (2x - 1) \tag{21}$$

A plot of αL vs. x is given in Fig. 7. It will be observed that in making the measurements, any discontinuity may be used as long as its coefficient of reflection does not vary as it is moved along the transmission line. Thus, if the reflection coefficient of the discontinuity is not unity, the transmission line beyond the discontinuity must be terminated in its characteristic impedance. Usually, any gradually increasing lossy termination will be satisfactory. It is observed that only three measurements are required for three positions of the discontinuity to determine each circle. However,

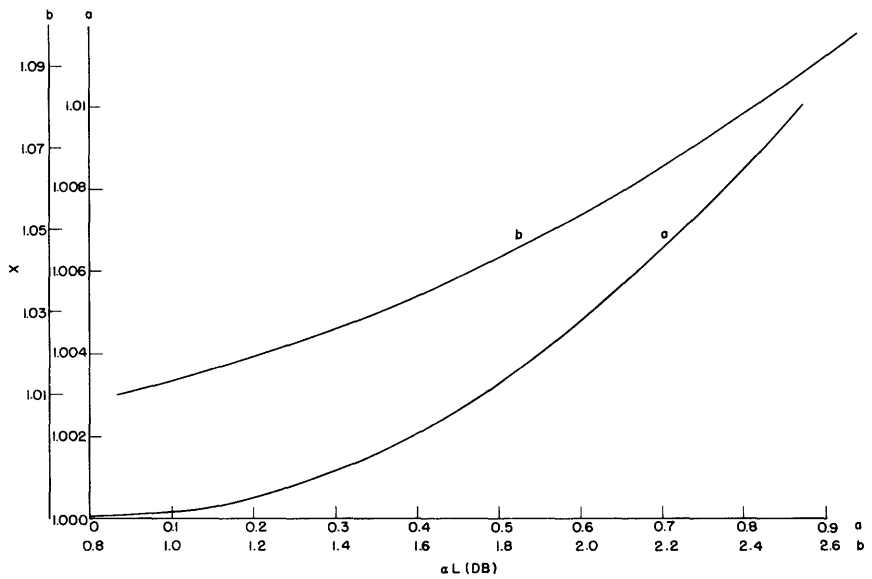

Fig. 13
The cross ratio, X, vs. attenuation.

to decrease experimental error and to insure a good distribution of data, at least five points should be plotted on the Smith chart for five positions of the discontinuity spaced equally along a half wavelength in the transmission line.

Thus, if the attenuation of a transmission line is desired, and measurements are to be made through any junction (such as connectors, adapters, cables, etc.), the attenuation may be determined by plotting two circles on a Smith chart in the usual manner and measuring $X = (D-C)(d+c)/Dd$. The attenuation for the distance L may then be obtained from Fig. 13. If the scattering matrix of the junction or of a discontinuity along a transmission line is desired, it may also be determined by a graphical analysis (15).

E. DESCRIPTION OF APPARATUS

Since most commercial plastics use Apoxy resin (loss factor of approximately 0.03 at S-band frequencies) for a binder, they were not used in the manufacture of the strip transmission line for the attenuation and wavelength measurements. Instead, the strip line was constructed by chemically depositing a thin layer of silver on both sides of a polystyrene sheet (16, 17). The silver layer was used as an electrode to electroplate copper to a thickness of 0.006 inch ± 0.001 inch. The polystyrene sheet was then cut to a width of 5 inches and a length of 26 inches. To make the structure rigid, the polystyrene sheet was glued to a quarter-inch steel plate of like dimension. The strip was milled, parallel to one side of the steel plate, from the copper on the free side of the polystyrene sheet, and a coaxial coupling was attached (Fig. 14). In order to decrease reflections, a gradually increasing lossy termination made of Thiokol PRI compound

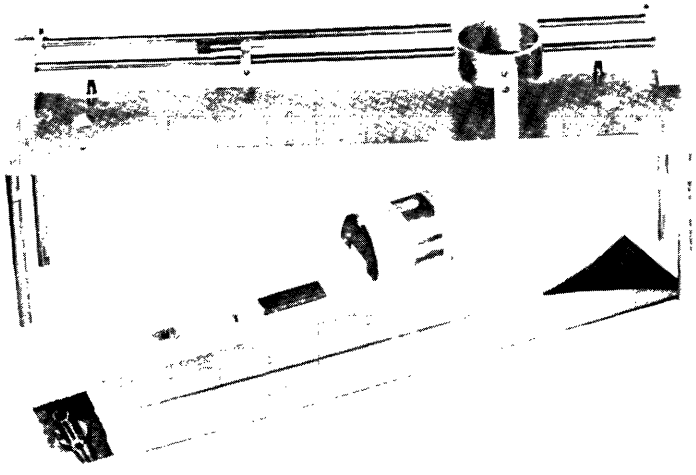

Fig. 14
Exploded view of the test bench and strip line.

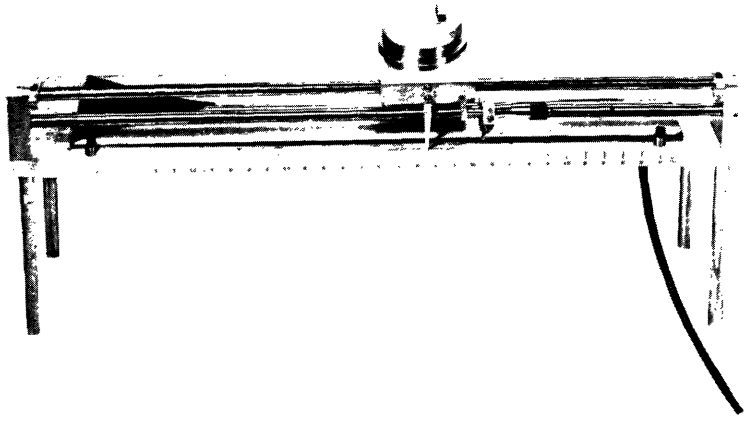

Fig. 15
Assembled view of the test bench with the strip line in place.

($K = 8.4$, $\tan \delta = 0.22$ at X-band frequencies) was placed on the strip line, as shown in Fig. 14.

For measurements of the strip line, a special test bench was designed to move accurately a discontinuity on the strip (Fig. 15). The discontinuities were made of silver plated brass slugs that were maintained in proper geometrical orientation, as well as in intimate contact with the strip, by a slug bar. A cylinder made of Eccofoam plastic, into which a short piece of X-band waveguide was fitted, securely held the slug bar. The cylinder was held by a brass collar that rode on a guide bar fixed parallel to the strip and moved by a millimeter micrometer. Behind the slug, a piece of Thiokol PRI compound was attached to the Eccofoam cylinder to insure that any reflections from the termination of the strip line would be absorbed and not interfere with the measurements. Thus, the discontinuity is isolated from the termination of the strip line.

References

1. G. Goubau, Surface waves and their application to transmission lines, J. Appl. Phys. 21, 11, 1119 (1950).
2. R. M Barrett, Etched sheets serve as microwave components, Electronics Magazine 25, 114 (1952).
3. E. G Fubini, W. E. Fromm, and H. S. Keen, New techniques for high-Q strip microwave components, Convention Record of the I. R. E., 1954 National Convention, 2, Part 8, p. 91.
4. M. Schetzen, Printed microwave systems, M. Sc. Thesis, Department of Electrical Engineering, M. I. T. (1954).
5. M. Arditi, Experimental determination of the properties of microstrip components, Elect. Commun. 30, 4, 283 (1953).
6. S. S. Attwood, Surface wave propagation over a coated plane conductor, J. Appl. Phys. 22, 4, 604 (1951).
7. H. M. Barlow and A. L. Cullen, Surface waves, Proc. Instn. Elect. Engrs., Part III, No. 68, p. 329 (1953).
8. R. B. Adler, Properties of guided waves on inhomogeneous cylindrical structures, Technical Report 102, Research Laboratory of Electronics, M. I. T. (1949).
9. H. B. Palmer, The capacitance of a parallel-plate capacitor by the Schwartz-Cristoffel transformation, Trans. Am. Inst. Elec. Engrs. 56, 3, 363 (1937).
10. J Hodgkinson, A note on a two-dimensional problem in electrostatics, The Quarterly Journal of Mathematics, Oxford Series, 9, 5-13 (1938).
11. R. D. Richtmyer, Dielectric resonators, J. Appl. Phys. 10, 6, 391 (1939).
12. F. Assadourian and E. Rimai, Simplified theory of microstrip transmission systems, Proc. Inst. Radio Engrs. 1651 (1952).
13. A. D. Berk, Cavities and waveguides with inhomogeneous and anisotropic media, D. Sc. Thesis, Department of Electrical Engineering, M. I. T. (1954).
14. R. V Churchill, Introduction to Complex Variables and Applications (McGraw-Hill Book Company, Inc., New York, 1948) p. 57.
15. J. E. Storer, L. S. Sheingold, and S. Stein, A simple graphical analysis of wave-guide junctions, Technical Report No. 160, Cruft Laboratory, Harvard University, August 1952.
16. New Advances in Printed Circuits, Miscellaneous Publication No. 192, Nov. 22, 1948, Nat. Bur. Standards.
17. Printed Circuit Techniques, Circular No. 468, Nov. 15, 1947, Nat. Bur. Standards.

APPENDIX I

DEFINITION OF NOTATION USED

In Appendices II-V some of the notation used for the electromagnetic field is not standard. As an aid to the reader, this appendix is devoted to a brief notation discussion.

In determining the field solutions for any system, the fundamental equations that must be solved subject to the boundary conditions are the Maxwell equations

$$\nabla \times E = -jk\zeta H$$

$$\nabla \times H = jk\eta E$$

where $k^2 = \omega\mu(\omega\epsilon - j\sigma)$, $\zeta^2 = \omega\mu/(\omega\epsilon - j\sigma)$, and $\eta = 1/\zeta$.

If the free mode solutions of a cylindrical structure of arbitrary cross section are desired, the solutions may be obtained in terms of the scalar potential functions Φ (for the E-modes) and ψ (for the H-modes) that satisfy the two-dimensional scalar Helmholtz equation

$$\nabla_T^2 \theta + P^2 \theta = 0 \tag{I-1}$$

In terms of these scalar functions, all the field quantities may be determined. Thus, for the E-waves

$$E_T = V(z)\, T_1^e (x, y) \tag{I-2}$$

$$E_z = L(z)\, \Phi(x, y) \tag{I-3}$$

where

$$T_1^e (x, y) = -\nabla_T \Phi(x, y) \tag{I-4}$$

The other field quantities for the E-mode may be determined as follows: From the equation

$$\nabla \cdot E = \nabla_T \cdot E_T + \frac{\partial}{\partial z} E_z = 0$$

we obtain, by the use of Eqs. I-1 through I-4

$$V(z)\, P^2 \Phi - j\, \gamma L(z)\, \Phi = 0$$

Thus

$$L(z) = \frac{P^2}{j\gamma} V(z) \tag{I-5}$$

The longitudinal component of Maxwell's equation

$$\nabla \times H = j\, k\eta E$$

may be written as

$$\nabla_T \times H_T = j\, k\eta E_z \vec{i}_z$$

where

$$H_T = I(z) \left[\vec{i}_z \times T_1^e(x, y)\right] \tag{I-6}$$

Upon substituting Eqs. I-1 through I-6 we obtain

$$I(z) \left[\nabla_T \cdot T_1^e(x, y)\right] = j\, k\eta E_z$$

$$I(z)\, P^2\, \Phi = k\eta \frac{P^2}{\gamma^2} \Phi\, V(z)$$

Thus

$$I(z) = \frac{k\eta}{\gamma} V(z)$$

The fields of the E-modes are therefore

$$E_T^e = V(z)\, T_1^e(x, y)$$

$$E_z = \frac{P^2}{j\gamma} V(z)\, \Phi(x, y)$$

$$H_T^e = \frac{k\eta}{\gamma} V(z)\, T_2^e(x, y)$$

where

$$T_2^e(x, y) = \vec{i}_z \times T_1^e(x, y)$$

$$T_1^e(x, y) = -\nabla_T \Phi$$

$$\gamma^2 = k^2 - P^2$$

and $\Phi(x, y)$ is a solution of

$$\nabla_T^2\, \Phi + P^2\, \Phi = 0$$

By a similar process, the fields may be obtained for the H-modes as

$$H_T^h = I(z)\, T_2^h(x, y)$$

$$H_z = \frac{P^2}{j\gamma} I(z)\, \psi(x, y)$$

$$E_T^h = \frac{\omega\mu}{\gamma} I(z)\, T_1^h(x, y)$$

where

$$T_1^h(x, y) = -\vec{i}_z \times T_2^h(x, y)$$

$$T_2^h(x, y) = -\nabla_T \psi$$

and $\psi(x, y)$ is a solution of

$$\nabla_T^2 \psi + P^2 \psi = 0$$

APPENDIX II

PROOF THAT THE ONLY TYPES OF FREE MODES POSSIBLE ON PARALLEL-WIRE TRANSMISSION LINES ARE TEM MODES

Consider an n-conductor system of arbitrary but constant cross section in homogeneous and simply connected space. If higher order modes are to exist, the equation that must be satisfied is the two-dimensional scalar Helmholtz equation

$$\nabla_T^2 \Phi + P^2 \Phi = 0 \tag{II-1}$$

with the boundary condition that, on the conducting surfaces, either $\Phi = 0$ (for E-waves) or $\partial\Phi/\partial n = 0$ (for H-waves).

From Green's first theorem in two dimensions we have

$$\int_A \left[\psi \nabla_T^2 \Phi + \nabla_T \Phi \cdot \nabla_T \psi\right] da = \oint_S \psi \nabla_T \Phi \cdot \vec{n}\, ds \tag{II-2}$$

Let $\Phi = \Phi$ and $\psi = \Phi^*$. From Eq. II-2

$$\int_A \left[\Phi^* \nabla_T^2 \Phi + ||\nabla_T \Phi||^2\right] da = \oint_S \Phi^* \partial\Phi/\partial n\, ds \tag{II-3}$$

Choose the area, A, to be the infinite cross section. Since the total energy in a cross section is finite, the fields will be zero at infinity. Also, either Φ or $\partial\Phi/\partial n$ is zero on the conducting surfaces. Thus

$$\oint_S \Phi^* \partial\Phi/\partial n\, ds = 0$$

and from Eq. II-3, therefore,

$$\int_A \Phi^* \nabla_T^2 \Phi\, da = -\int_A ||\nabla_T \Phi||^2\, da \tag{II-4}$$

By substituting the value of $\nabla_T^2 \Phi$ from Eq. II-1 and solving Eq. II-4 for P^2, one obtains

$$P^2 = \frac{\int_A ||\nabla_T \Phi||^2\, da}{\int_A ||\Phi||^2\, da} \tag{II-5}$$

Equation II-5 states that if higher order free modes are to exist, P^2 must be a positive real quantity. However, in order for the total energy over a cross section to be finite, P must be imaginary, and thus P^2 must be negative. But this is in contradiction

to the requirements imposed upon P^2 by Eq. II-5. Thus, no higher order free modes may exist. It is observed that the TEM wave satisfies the Laplace equation

$$\nabla_T^2 \Phi = 0$$

where Φ is a constant on the conducting surfaces; thus, the proof given above is not valid for the TEM wave.

It has therefore been proved that the only types of free modes possible on any n-conductor system of arbitrary but constant cross section in homogeneous, simply connected space are TEM modes.

APPENDIX III

THEORETICAL ANALYSIS OF THE STRIP TRANSMISSION LINE

Since the strip represents a discontinuous boundary condition to be satisfied, the solution for the fields will be obtained by first solving for the fields that would be caused by a sinusoidal current distribution on the surface of the dielectric. A Fourier integral of all such sinusoidal currents will then be formed so that it represents the fields caused by a current which is nonzero only over the region occupied by the strip.

In the analysis, the following assumptions will be made:

(1) The ground plane and the dielectric sheet are infinite in extent.

(2) The strip is very narrow as compared with a wavelength.

(3) The strip is infinitesimally thin.

The solution will be exact for an infinitesimally thin wire and approximate for a strip.

Consider the system shown in Fig. III-1.

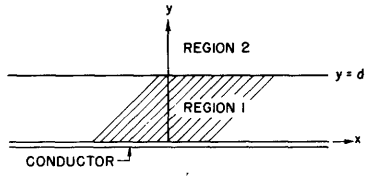

Fig. III-1
Strip transmission line.

Assume a current density to exist on the interface between regions 1 and 2 (plane of y = d).

$$K(x, z) = \vec{i}_z K_z \cos \alpha x \, e^{-j\gamma z} \tag{III-1}$$

The current density, K(x, z), will generate H-E waves which may be expressed as a linear combination of E- and H-waves. Thus, in the notation developed in Appendix I, for E-waves

$$E_T^e = V(z) \, T_1^e(x, y) \tag{III-2}$$

$$E_z = P^2/j\gamma \, V(z) \, \Phi(x, y) \tag{III-3}$$

$$H_T^e = \omega\epsilon/\gamma \, V(z) \, T_2^e(x, y) \tag{III-4}$$

where

$$T_2^e(x, y) = \vec{i}_z \times T_1^e(x, y) \tag{III-5}$$

$$T_1^e(x, y) = -\nabla_T \, \Phi(x, y) \tag{III-6}$$

$$V(z) = N\, e^{-j\gamma z} \tag{III-7}$$

and for H-waves

$$H_T^h = I(z)\, T_2^h(x, y) \tag{III-8}$$

$$H_z = P^2/j\gamma\, I(z)\, \psi(x, y) \tag{III-9}$$

$$E_T^h = \omega\mu/\gamma\, I(z)\, T_1^h(x, y) \tag{III-10}$$

where

$$T_1^h(x, y) = T_2^h(x, y) \times \vec{i}_z \tag{III-11}$$

$$T_2^h(x, y) = -\nabla_T\, \psi(x, y) \tag{III-12}$$

$$I(z) = N\, e^{-j\gamma z} \tag{III-13}$$

where N is an arbitrary constant and either Φ or ψ satisfies the Helmholtz equation.

Since $\vec{n} \times E = 0$ on the conductor (plane of $y = 0$), $\Phi(x, y)$ must have a $\sin \beta_1 y$ dependence in region 1. Also, since $\partial/\partial n(\vec{n} \times H) = 0$ on the conductor, $\psi(x, y)$ must have a $\cos \beta_1 y$ dependence in region 1. Thus, we may write

$$\Phi_1(x, y) = A \cos \alpha x \sin \beta_1 y \qquad y \leqslant d \tag{III-14}$$

$$\Phi_2(x, y) = B \cos \alpha x \exp[-(y-d)\, \beta_2] \qquad y \geqslant d \tag{III-15}$$

$$\psi_1(x, y) = C \sin \alpha x \cos \beta_1 y \qquad y \leqslant d \tag{III-16}$$

$$\psi_2(x, y) = D \sin \alpha x \exp[-(y-d)\, \beta_2] \qquad y \geqslant d \tag{III-17}$$

α and γ are the same for both regions and are given by the exciting current; β will be different.

$$\gamma^2 = k^2 - P^2$$

$$P^2 = \alpha^2 + \beta^2$$

$$k^2 = \omega^2\, \mu\epsilon$$

To determine the coefficients A, B, C, and D, we will use the boundary conditions that, at $y = d$,

$$H_{z_1} = H_{z_2} \tag{III-18}$$

$$E_{z_1} = E_{z_2} \tag{III-19}$$

$$E_{x_1} = E_{x_2} \tag{III-20}$$

$$H_{x_1} - H_{x_2} = K(x, z) \cdot \vec{i}_z \tag{III-21}$$

From Eqs. III-9, III-16, and III-17, we have, at y = d

$$H_{z_1} = P_1^2/j\gamma\ C \sin \alpha x \cos \beta_1 d$$

$$H_{z_2} = P_2^2/j\gamma\ D \sin \alpha x$$

Thus, upon substituting into Eq. III-18,

$$D = (P_1/P_2)^2\ C \cos \beta_1 d \tag{III-22}$$

Now, from Eqs. III-3, III-14, and III-15, we have, at y = d

$$E_{z_1} = P_1^2/j\gamma\ A \cos \alpha x \sin \beta_1 d \tag{III-23a}$$

$$E_{z_2} = P_2^2/j\gamma\ B \cos \alpha x \tag{III-23b}$$

Thus, upon substitution into Eq. III-19,

$$B = (P_1/P_2)^2\ A \sin \beta_1 d \tag{III-23}$$

From Eq. III-20, we have, at y = d

$$E^h_{x_1} + E^e_{x_1} = E^h_{x_2} + E^e_{x_2} \tag{III-24}$$

Now, however,

$$E^h_x = E^h_T \cdot \vec{i}_x$$

and thus from Eqs. III-10, III-11, and III-12, we have

$$E^h_x = \omega\mu/\gamma\ I(z)\ \partial\psi/\partial y \tag{III-25}$$

Also, from Eqs. III-2 and III-6

$$E^e_x = -V(z)\ \partial\Phi/\partial x \tag{III-26}$$

Thus, by substituting Eqs. III-25 and III-26 into III-24 we have, at y = d

$$\omega\mu/\gamma\ I(z)\ \partial\psi_1/\partial y + V(z)\ \partial\Phi_1/\partial x = \omega\mu/\gamma\ I(z)\ \partial\psi_2/\partial y + V(z)\ \partial\Phi_2/\partial x \tag{III-27}$$

Thus, by substituting Eqs. III-14 through III-17 into III-27, remembering that V(z) = I(z),

there results with the use of Eqs. III-22 and III-23

$$B\,\alpha\left[\left(\frac{P_2}{P_1}\right)^2 - 1\right] + D\,\frac{\omega\mu\beta_1}{\gamma}\left[\left(\frac{P_2}{P_1}\right)^2 \tan\beta_1 d - \frac{\beta_2}{\beta_1}\right] = 0 \tag{III-28}$$

To obtain the other relation between B and D, use will be made of the boundary condition specified by Eq. III-21. From this equation we have

$$H^e_{x_1} + H^h_{x_1} - H^e_{x_2} - H^h_{x_2} = K \cdot \vec{i}_z \tag{III-29}$$

Now, from Eqs. III-4, III-5, and III-6

$$H^e_x = H^e_T \cdot \vec{i}_x = \omega\epsilon/\gamma\; V(z)\; \partial\Phi/\partial y \tag{III-30}$$

And also, from Eqs. III-8 and III-12

$$H^h_x = H^h_T \cdot \vec{i}_x = -I(z)\; \partial\psi/\partial x \tag{III-31}$$

Thus, upon substitution of Eqs. III-1, III-30, and III-31 into III-29, we have, at y = d

$$\omega\epsilon_1/\gamma\; \partial\Phi_1/\partial y - \partial\psi_1/\partial x - \omega\epsilon_2/\gamma\; \partial\Phi_2/\partial y + \partial\psi_2/\partial x = K_z \cos\alpha x \tag{III-32}$$

Thus, by substituting Eqs. III-14 through III-17 into III-32 there results with the use of Eqs. III-22 and III-23

$$B\,\frac{\omega\epsilon_1\beta_1}{\gamma}\left[\left(\frac{P_2}{P_1}\right)^2 \operatorname{ctn}\beta_1 d + \frac{\epsilon_2\beta_2}{\epsilon_1\beta_1}\right] - D\,\alpha\left[\left(\frac{P_2}{P_1}\right)^2 - 1\right] = K_z \tag{III-33}$$

We now have two equations, Eq. III-28 and Eq. III-33, involving only B and D. These may be solved for B resulting in the equation

$$B = \frac{K_z\,\dfrac{\omega\mu\beta_1}{\gamma}\left[\left(\dfrac{P_2}{P_1}\right)^2 \tan\beta_1 d - \dfrac{\beta_2}{\beta_1}\right]}{\alpha^2\left[\left(\dfrac{P_2}{P_1}\right)^2 - 1\right]^2 + \dfrac{\omega^2\mu\epsilon_1\beta_1^2}{\gamma^2}\left[\left(\dfrac{P_2}{P_1}\right)^2 \tan\beta_1 d - \dfrac{\beta_2}{\beta_1}\right]\left[\left(\dfrac{P_2}{P_1}\right)^2 \operatorname{ctn}\beta_1 d + \dfrac{\epsilon_2\beta_2}{\epsilon_1\beta_1}\right]} \tag{III-34}$$

We have assumed, in this derivation so far, that Φ_2 and ψ_2 satisfy the Helmholtz equation

$$\nabla_T^2\,\theta_2 + P_2^2\,\theta_2 = 0$$

Since the fields in region 2 will decay, P_2^2 will be found to be a real negative quantity. It will be convenient, however, to redefine P_2^2 so that it is a positive real quantity. Therefore, let

$$P_2^2 = -P_3^2$$

The Helmholtz equation in region 2 thus becomes

$$\nabla_T^2 \theta_2 - P_3^2 \theta_2 = 0$$

and

$$\gamma^2 = k_1^2 - P_1^2 = k_2^2 + P_3^2$$

where

$$P_1^2 = \beta_1^2 + \alpha^2$$

$$P_2^2 = \beta_2^2 - \alpha^2$$

We now observe that for the free modes of the system

$$k_2 \leqslant \gamma \leqslant k_1 \tag{III-35}$$

where

$$k^2 = \omega^2 \mu \epsilon$$

Equation III-35 will be true for the free modes of any open boundary structure.

We may now rewrite Eq. III-34 in terms of P_3. Thus

$$B = \frac{-K_z \dfrac{\omega\mu\beta_1}{\gamma}\left[\left(\dfrac{P_3}{P_1}\right)^2 \tan \beta_1 d + \dfrac{\beta_2}{\beta_1}\right]}{\alpha^2\left[\left(\dfrac{P_3}{P_1}\right)^2 + 1\right]^2 + \dfrac{k_1^2\beta_1^2}{\gamma^2}\left[\left(\dfrac{P_3}{P_1}\right)^2 \tan \beta_1 d + \dfrac{\beta_2}{\beta_1}\right]\left[\left(\dfrac{P_3}{P_1}\right)^2 \operatorname{ctn} \beta_1 d - \dfrac{\epsilon_2\beta_2}{\epsilon_1\beta_1}\right]} \tag{III-36}$$

For the strip transmission system, it will be assumed that the strip width is much less than a wavelength, so that the current may be assumed to be constant across it. It will further be assumed that the current in the strip flows only in the longitudinal direction (in the z-direction). We note that under these restrictions, the current, plotted as a function of x, will appear as a rectangular pulse which may be represented as a Fourier integral.

Let the strip width be 2δ. Then the current

$$K_z = \begin{Bmatrix} 0 & -\infty < x < -\delta \\ K & -\delta < x < \delta \\ 0 & \delta < x < \infty \end{Bmatrix}$$

$$K_z = \int_{-\infty}^{\infty} K_z(\alpha) \cos \alpha x \, d\alpha$$

Thus

$$K_z(\alpha) = \frac{1}{2\pi} \int_{-\infty}^{\infty} K_z \cos \alpha x \, dx$$

$$K_z(\alpha) = \frac{K\delta}{\pi} \frac{\sin \alpha\delta}{\alpha\delta} \tag{III-37}$$

It is now required that the boundary condition that $\vec{n} \times E = 0$ on the strip be satisfied. However, since the strip width has been assumed to be much less than a wavelength, it will suffice to make $E_z = 0$ only at the center of the strip ($x = 0$, $y = d$) instead of over the range $-\delta \leqslant x \leqslant \delta$. It will thus be required that

$$\int_{-\infty}^{\infty} E_z(0, d) \, d\alpha = 0$$

Substituting Eq. III-23b, there results

$$\int_{-\infty}^{\infty} P_2^2/j\gamma \, B \, d\alpha = 0$$

However, since $P_2^2/j\gamma$ is not a function of α and noting from Eq. III-36 that B is an even function of α, we need only require that

$$\int_{0}^{\infty} B \, d\alpha = 0 \tag{III-38}$$

Thus, substituting Eqs. III-36 and III-37 into Eq. III-38, we find that the determinantal equation for the strip transmission line is

$$\int_{0}^{\infty} \frac{\beta_1 \left[\left(\frac{P_3}{P_1}\right)^2 \tan \beta_1 d + \frac{\beta_2}{\beta_1}\right] \frac{\sin \alpha\delta}{\alpha\delta} \, d\alpha}{\alpha^2 \left[\left(\frac{P_3}{P_1}\right)^2 + 1\right]^2 + \frac{k_1^2 \beta_1^2}{\gamma^2} \left[\left(\frac{P_3}{P_1}\right)^2 \tan \beta_1 d + \frac{\beta_2}{\beta_1}\right] \left[\left(\frac{P_3}{P_1}\right)^2 \operatorname{ctn} \beta_1 d - \frac{\epsilon_2 \beta_2}{\epsilon_1 \beta_1}\right]} = 0 \tag{III-39}$$

Equation III-39 determines those values of the free mode propagation constants, $\gamma = \gamma_n$, for the strip transmission line, where

$$\gamma^2 = k_1^2 - P_1^2$$

$$\gamma^2 = k_2^2 + P_3^2$$

$$P_1^2 = \alpha^2 + \beta_1^2 > 0$$

$$P_3^2 = \beta_2^2 - \alpha^2 > 0$$

$$k^2 = \omega^2 \mu \epsilon$$

The fields are then given by:

For $y < d$

$$E_{z_1} = \frac{N P_1^2}{j\gamma_n} \exp(-j\gamma_n z) \int_{-\infty}^{\infty} A \cos \alpha x \sin \beta_1 y \, d\alpha \tag{III-40a}$$

$$H_{z_1} = \frac{N P_1^2}{j\gamma_n} \exp(-j\gamma_n z) \int_{-\infty}^{\infty} C \sin \alpha x \cos \beta_1 y \, d\alpha \tag{III-40b}$$

$$E_{x_1} = N \exp(-j\gamma_n z) \int_{-\infty}^{\infty} \left\{ \frac{\omega\mu\beta_1}{\gamma_n} C + \alpha A \right\} \sin \alpha x \sin \beta_1 y \, d\alpha \tag{III-40c}$$

$$H_{x_1} = N \exp(-j\gamma_n z) \int_{-\infty}^{\infty} \left\{ \frac{\omega\epsilon_1\beta_1}{\gamma_n} A - \alpha C \right\} \cos \alpha x \cos \beta_1 y \, d\alpha \tag{III-40d}$$

$$E_{y_1} = N \exp(-j\gamma_n z) \int_{-\infty}^{\infty} \left\{ \frac{\omega\mu_1\alpha}{\gamma_n} C - \beta_1 A \right\} \cos \alpha x \cos \beta_1 y \, d\alpha \tag{III-40e}$$

$$H_{y_1} = N \exp(-j\gamma_n z) \int_{-\infty}^{\infty} \left\{ \frac{\omega\epsilon_1\alpha}{\gamma_n} A + \beta_1 C \right\} \sin \alpha x \cos \beta_1 y \, d\alpha \tag{III-40f}$$

and for $y > d$

$$E_{z_2} = -\frac{N P_3^2}{j\gamma_n} \exp(-j\gamma_n z) \int_{-\infty}^{\infty} B \cos \alpha x \exp[-(y-d)\beta_2] \, d\alpha \tag{III-41a}$$

$$H_{z_2} = -\frac{N P_3^2}{j\gamma_n} \exp(-j\gamma_n z) \int_{-\infty}^{\infty} D \sin \alpha x \exp[-(y-d)\beta_2] \, d\alpha \tag{III-41b}$$

$$E_{x_2} = N \exp(-j\gamma_n z) \int_{-\infty}^{\infty} \left\{ \frac{\omega\mu_2\beta_2}{\gamma_n} D + \alpha B \right\} \sin \alpha x \exp[-(y-d)\beta_2] \, d\alpha \tag{III-41c}$$

$$H_{x_2} = -N \exp(-j\gamma_n z) \int_{-\infty}^{\infty} \left\{ \frac{\omega\epsilon_2\beta_2}{\gamma_n} B - \alpha D \right\} \cos \alpha x \exp[-(y-d)\beta_2] \, d\alpha \tag{III-41d}$$

$$E_{y_2} = N \exp(-j\gamma_n z) \int_{-\infty}^{\infty} \left\{ \frac{\omega\mu_2\alpha}{\gamma_n} D + \beta_2 B \right\} \cos \alpha x \exp[-(y-d)\beta_2] \, d\alpha \tag{III-41e}$$

$$H_{y_2} = N \exp(-j\gamma_n z) \int_{-\infty}^{\infty} \left\{ \frac{\omega\epsilon_2\alpha}{\gamma_n} B + \beta_2 D \right\} \sin \alpha x \exp[-(y-d)\beta_2] \, d\alpha \tag{III-41f}$$

where, from Eqs. III-22, III-23, and III-28

$$A = -(P_3/P_1)^2 B \csc \beta_1 d \tag{III-42a}$$

$$C = -\frac{\gamma_n}{\omega\mu}\left(\frac{P_3}{P_1}\right)^2 \left[\left(\frac{P_3}{P_1}\right)^2 + 1\right] \frac{\alpha \sec \beta_1 d}{\beta_1 \left[\left(\frac{P_3}{P_1}\right)^2 \tan \beta_1 d + \frac{\beta_2}{\beta_1}\right]} B \tag{III-42b}$$

$$D = \frac{\gamma_n}{\omega\mu}\left[\left(\frac{P_3}{P_1}\right)^2 + 1\right] \frac{\alpha B}{\beta_1 \left[\left(\frac{P_3}{P_1}\right)^2 \tan \beta_1 d + \frac{\beta_2}{\beta_1}\right]} \tag{III-42c}$$

and B is given by Eq. III-36.

APPENDIX IV

THE CHARACTERISTIC IMPEDANCE OF THE STRIP TRANSMISSION LINE

The characteristic impedance of the strip transmission line may be defined as

$$Z_o = \frac{V}{I}$$

where I is defined as the total longitudinal current in the strip, and V is the integral of the electric field from the ground plane to the strip along the axis of symmetry of the cross section. Thus

$$Z_o = \frac{\int_0^d E_y(0, y)\, dy}{\int_{-\delta}^{\delta} K(x)\, dx} \tag{IV-1}$$

Since the current density was assumed constant across the strip,

$$\int_{-\delta}^{\delta} K(x)\, dx = 2\delta K \tag{IV-2}$$

From Eq. III-40e of Appendix III, let N = 1; then

$$E_{y_1}(0, y) = \int_{-\infty}^{\infty} \left\{\frac{\omega\mu\alpha}{\gamma_n} C - \beta_1 A\right\} \cos \beta_1 y\, d\alpha \tag{IV-3}$$

Thus

$$V = \int_{-\infty}^{\infty} \left\{\left[\frac{\omega\mu\alpha}{\gamma_n} C - \beta_1 A\right] \int_0^d \cos \beta_1 y\, dy\right\} d\alpha$$

$$= \int_{-\infty}^{\infty} \left\{\frac{\omega\mu\alpha}{\beta_1 \gamma_n} C - A\right\} \sin \beta_1 d\, d\alpha$$

However, from Eqs. III-42a and III-38 of Appendix III

$$\int_{-\infty}^{\infty} A \sin \beta_1 d\, d\alpha = 0$$

Thus

$$V = \int_{-\infty}^{\infty} \frac{\omega\mu\alpha}{\beta_1 \gamma_n} C \sin \beta_1 d\, d\alpha \tag{IV-4}$$

Equation III-42b in Appendix III could be directly substituted into Eq. IV-4. However, since it was established in Section III that the phase velocity of the H-E mode is not a function of frequency, we may write for the H-E mode

$$\gamma^2 = \omega^2 \mu \epsilon_e \tag{IV-5}$$

where ϵ_e is defined as an "effective" permittivity. Thus, by use of this definition of γ

$$\left(\frac{P_3}{P_1}\right)^2 = \frac{\gamma^2 - k_2^2}{k_1^2 - \gamma^2} = \frac{\chi_e}{\chi_1 - \chi_e} \tag{IV-6}$$

where χ_e is the "effective" electric susceptibility and χ_1 is the electric susceptibility of the dielectric sheet.

By the use of this definition, the equation for V becomes, after substituting Eqs. III-42b, III-36, and III-37 of Appendix III,

$$V = \left[\frac{\chi_e \chi_1 K_z}{\pi(\chi_1 - \chi_e)^2} (\mu/\epsilon_e)^{1/2}\right]$$

$$\int_{-\infty}^{\infty} \frac{\dfrac{\tan \beta_1 d}{\beta_1} \dfrac{\sin \alpha\delta}{\alpha} d\alpha}{\left(\dfrac{\chi_1}{\chi_1 - \chi_e}\right)^2 + \dfrac{\epsilon_1 \beta_1^2}{\epsilon_e \alpha^2} \left[\dfrac{\chi_e}{\chi_1 - \chi_e} \tan \beta_1 d + \dfrac{\beta_2}{\beta_1}\right] \left[\dfrac{\chi_e}{\chi_1 - \chi_e} \operatorname{ctn} \beta_1 d - \dfrac{\epsilon_2 \beta_2}{\epsilon_1 \beta_1}\right]} \tag{IV-7}$$

However,

$$(\mu/\epsilon_e)^{1/2} = \frac{120\pi}{(K_e)^{1/2}}$$

where K_e is the "effective" dielectric constant = $\chi_e + 1$. Thus, upon substituting Eqs. IV-7 and IV-2 into Eq. IV-1, the expression for the characteristic impedance becomes

$$Z_o = \left[\frac{120}{(K_e)^{1/2}} \frac{\chi_e \chi_1}{(\chi_1 - \chi_e)^2}\right]$$

$$\int_{0}^{\infty} \frac{\dfrac{\tan \beta_1 d}{\beta_1} \dfrac{\sin \alpha\delta}{\alpha\delta} d\alpha}{\left(\dfrac{\chi_1}{\chi_1 - \chi_e}\right)^2 + \dfrac{\epsilon_1 \beta_1^2}{\epsilon_e \alpha^2} \left[\dfrac{\chi_e}{\chi_1 - \chi_e} \tan \beta_1 d + \dfrac{\beta_2}{\beta_1}\right] \left[\dfrac{\chi_e}{\chi_1 - \chi_e} \operatorname{ctn} \beta_1 d - \dfrac{\epsilon_2 \beta_2}{\epsilon_1 \beta_1}\right]} \tag{IV-8}$$

where

$$\beta_1^2 = P_1^2 - \alpha^2 = \omega^2\mu(\epsilon_1 - \epsilon_e) - \alpha^2$$

$$\beta_2^2 = P_3^2 + \alpha^2 = \omega^2\mu(\epsilon_e - \epsilon_2) + \alpha^2$$

Since the integrand is an even function of α, twice the integral from zero to infinity has been taken.

Equation IV-8 thus determines the characteristic impedance for the H-E mode of the strip transmission line. At zero frequency, the characteristic impedance is thus

$$Z_o = \left[\frac{120}{(K_e)^{1/2}} \frac{\chi_e \chi_1}{(\chi_1 - \chi_e)^2}\right] \int_0^\infty \frac{\frac{\tanh \alpha d}{\alpha} \frac{\sin \alpha\delta}{\alpha\delta} d\alpha}{\left(\frac{\chi_1}{\chi_1 - \chi_e}\right)^2 + \frac{K_1}{K_e}\left[\frac{\chi_e}{\chi_1 - \chi_e} \tanh \alpha d - 1\right]\left[\frac{1}{K_1} - \frac{\chi_e}{\chi_1 - \chi_e} \operatorname{ctnh} \alpha d\right]} \tag{IV-9}$$

Since N has been arbitrarily set equal to one, the zero frequency characteristic impedance as defined by Eq. IV-9 will differ, by a normalization factor, from that calculated by the equation

$$Z_o = (L/C)^{1/2}$$

where L is the inductance per unit length and C is the capacitance per unit length of the strip transmission line.

APPENDIX V

A VARIATIONAL APPROACH TO THE STRIP TRANSMISSION LINE*

Let the electric field, $\mathscr{E}$, and the magnetic field, $\mathscr{H}$, be

$$\mathscr{E} = E(x, y)\, e^{j(\omega t - \gamma z)}$$

$$\mathscr{H} = H(x, y)\, e^{j(\omega t - \gamma z)}$$

A variational expression for the propagation constant, γ, may then be written in terms of E and H (13).

$$\gamma = \frac{\omega \int_S \epsilon\, |E|^2\, da + \omega \int_S \mu |H|^2\, da + j \int_S E^* \cdot \nabla \times H\, da - j \int_S H^* \cdot \nabla \times E\, da}{\int_S H^* \cdot \vec{i}_z \times E\, da - \int_S E^* \cdot i_z \times H\, da} \tag{V-1}$$

where, from Maxwell's equations

$$\nabla \times E - j\gamma\, \vec{i}_z \times E = -j\omega\mu H \tag{V-2}$$

$$\nabla \times H - j\gamma\, \vec{i}_z \times H = j\omega\epsilon E \tag{V-3}$$

Since, by the nature of a variational expression, the percentage error in γ will be considerably less than the percentage error in the trial field, we will assume a plane wave as the trial field.

Thus, let

$$E = -\nabla\Phi \tag{V-4}$$

and therefore

$$H = -\gamma/\omega\mu\, \vec{i}_z \times \nabla\Phi \tag{V-5}$$

Upon substituting Eqs. V-4 and V-5 into Eq. V-1,

$$\gamma = \frac{\omega\epsilon_o \int_S ||\nabla\Phi||^2\, da + \omega\chi\epsilon_o \int_s ||\nabla\Phi||^2\, da + \frac{\gamma^2}{\omega\mu} \int_S ||i_z \times \nabla\Phi||^2\, da}{\frac{\gamma}{\omega\mu} \int_S ||i_z \times \nabla\Phi||^2\, da + \frac{\gamma}{\omega\mu} \int_S ||\nabla\Phi||^2\, da} \tag{V-6}$$

where S is the total cross sectional area, s is that portion of the cross sectional area occupied by the dielectric sheet, and $\chi = K-1$ is the electric susceptibility of the dielectric sheet. However, since

---

*I wish to thank Mr. A. D. Berk, of this Laboratory, for suggesting the application of the variation principle to the strip transmission line.

$$\int_S ||i_z \times \nabla\Phi||^2 \, da = \int_S ||\nabla\Phi||^2 \, da$$

Eq. V-6 may be written as

$$\gamma^2 = k_o^2 \left[1 + \chi \frac{\int_s ||\nabla\Phi||^2 \, da}{\int_S ||\nabla\Phi||^2 \, da} \right] \tag{V-7}$$

where $k_o^2 = \omega^2 \mu \epsilon_o$. It is observed from Eq. V-7 that the propagation constant may be expected to be proportional to frequency and thus may be written as

$$\gamma^2 = \omega^2 \mu \epsilon_e$$

where ϵ_e is defined as an "effective" permittivity. In terms of this definition, Eq. V-7 may be rewritten as

$$\chi_e = \chi \frac{\int_s ||\nabla\Phi||^2 \, da}{\int_S ||\nabla\Phi||^2 \, da} \tag{V-8}$$

where χ_e is the "effective" electric susceptibility. From Eq. V-8 we may expect that for small electric susceptibility of the dielectric sheet, χ_e will increase linearly with χ.

Since the stored electric energy per unit length is

$$W_e = \frac{1}{2} \int_S \epsilon \, E \cdot E^* \, da$$

we may write

$$\int_s ||\nabla\Phi||^2 \, da = \frac{2W_1}{\epsilon} \tag{V-9}$$

$$\int_S ||\nabla\Phi||^2 \, da = \frac{2W_1}{\epsilon} + \frac{2W_o}{\epsilon_o} \tag{V-10}$$

where W_1 is the stored electric energy per unit length in the region occupied by the dielectric sheet, and W_o is the stored electric energy per unit length in the region above the dielectric sheet. Substituting Eqs. V-9 and V-10 into Eq. V-8 the relation

$$\frac{W_1}{W_1 + W_o} = \frac{K\chi_e}{\chi K_e} \tag{V-11}$$

is obtained where $\chi = K - 1$ is the electric susceptibility of the dielectric sheet, and $\chi_e = K_e - 1$ is the "effective" electric susceptibility of the H-E mode.

Equation V-11 is an approximate expression for the ratio of the energy stored in the dielectric region to the total stored energy of the H-E mode.